SCIENTIFIC REPORTS

OPEN

SUBJECT AREAS:
SOLAR CELLS
ELECTRONIC MATERIALS

Received
25 July 2013

Accepted
16 December 2013

Published
14 January 2014

Correspondence and requests for materials should be addressed to J.N.W. (jnwang@ecust.edu.cn)

Influence of Preferred Orientation on the Electrical Conductivity of Fluorine-Doped Tin Oxide Films

Jian Tao Wang[1], Xiang Lei Shi[1], Wei Wei Liu[1], Xin Hua Zhong[1], Jian Nong Wang[1], Leo Pyrah[2], Kevin D. Sanderson[2], Philip M. Ramsey[2], Masahiro Hirata[3] & Keiko Tsuri[3]

[1]Nanomaterials-X Research Center, School of Mechanical and Power Engineering and School of Chemistry and Molecular Engineering, East China University of Science and Technology, 130 Meilong Road, Shanghai 200237, P. R. of China, [2]Pilkington Technology Management Limited, Pilkington European Technical Centre, Hall Lane, Lathom L40 5UF, United Kingdom, [3]Nippon Sheet Glass Co., Ltd., R&D, 2-13-12 Konoike, Itami, Hyogo 664-8520, Japan.

Current development of high-performance transparent conductive oxide (TCO) films is limited with tradeoff between carrier mobility and concentration since none of them can be improved without sacrificing the other. In this study, we prepare fluorine doped tin oxide (FTO) films by chemical vapor deposition with inclusions of different additives and report that the mobility can be varied from 0.65 to 28.5 $cm^2 V^{-1} s^{-1}$ without reducing the achieved high carrier concentration of 4×10^{20} cm^{-3}. Such an increase in mobility is shown to be clearly associated with the development of (200) preferred orientation (PO) but concurrent degradation of (110) PO in films. Thus, at a constant high carrier concentration, the electrical conductivity can be improved via carrier mobility simply by PO control. Such a one-step approach avoiding conventional post-deposition treatment is suggested for developing next-generation FTO as well as other TCO films with better than ever conductivities.

Thin films made from transparent conducting oxides (TCOs) show high visible wavelength transparency and electrical conductivity at the same time, and have already been used in many devices requiring a transparent contact[1]. Typical examples include light emitting diodes[2,3], solar cells[4], flat panel displays[5], low emissivity windows[6], and electrochromatic, or smart, windows[7,8]. In addition, TCOs also offer an attractive prospect for completely transparent electronic display screens or even energy generation from photovoltaic cells invisibly incorporated into the windows of office buildings[9]. For most of these applications, TCOs are required to possess high transparency and high conductivity at the same time. However, the optical and electrical properties are inversely linked to each other, and neither one of them can be decoupled and changed independently without affecting the other. This is the main challenge towards improvement of current materials and development of a new range of high performance TCOs for increased functionality and performance.

Current good transparent conductors are obtained by creating electron degeneracy in wide band gap (>3 eV) oxides by controllably introducing non-stoichiometry and/or appropriate dopants[10]. For example, in fluorine doped tin oxide (FTO), F substitutes for O^{2-} and acts as an electron donor, resulting in an n-type degenerate semiconductor[11,12]. The creation of defects such as oxygen vacancies, and substitutional and interstitial impurities gives rise to the donation of electrons to the conduction band and provides charge carriers for the flow of electric current. The electrical conductivity κ, which is the reciprocal of resistivity ρ, has a relationship to the charge carrier density N and mobility μ as $\kappa = 1/\rho \propto N\mu$[1]. Apparently, ρ can be decreased by increasing N, by means of doping for example. A high N level, however, has the drawback of reducing the film transparency, as N is inversely related to the plasma wavelength λ_p as $\lambda_p \propto 1/N^{1/2}$. This becomes especially relevant if the electron concentration exceeds 10^{20} cm^{-3}, when absorption by free carriers or by metal-like reflection starts to become a restricting factor. Therefore, for applications where transparency is a critical parameter, such as solar cells, reduction in ρ must be achieved by increasing μ while maintaining a sufficiently high N ($\geq 10^{20}$ cm^{-3}) and transparency[13].

Several approaches have been used to increase μ for TCO thin films[1,14]. These approaches, proposed and practiced mainly for impurity doped In_2O_3 and CdO, include heat treatment, choice of deposition technique, use of substrate as well as controlling doping. Heat treatment after deposition was observed to increase the grain size, and thus improve the crystalline structure and the electron mobility of poorly crystallized TCO films[15]. However, such heat treatment also decreases the carrier density. The advantage of choosing deposition methods involving

highly energetic particles is a possible increase of the grain size and thus improvement of crystalline structures of TCO films[15]. Nevertheless, an excessive transfer of momentum could damage the films and thus reduce the mobility. Use of highly oriented substrates such as sapphire[16], zirconia(100)[17], and MgO(100)[18] for crystal growth is known to increase the mobility by improving the crystallinity of TCO thin films. But, these highly oriented substrates are relatively costly and little suitable for large areas. Control of doping is particularly used for mobility enhancement. Relatively high mobilities have been achieved in ZnO by Al doping, in CdO by doping with In, Sc, Y and Ti, and in In_2O_3 by doping with Mo, Ti, W, Zr, and Gd[1]. But, all these dopants limit the mobility by ionized impurity scattering when carrier densities are greater than 10^{20} cm^{-3}.

Some attempts have also been made to achieve high mobility for FTO films. Notably, use of tin tetrachloride as Sn precursor was favorable for high mobility (60 $cm^2V^{-1}s^{-1}$)[19,20]. Use of a temperature gradient during deposition led to a mobility of 77.5 $cm^2V^{-1}s^{-1}$ for films with low carrier concentrations ($\sim10^{20}$ cm^{-3}) and high thicknesses (1000–1500 nm)[20]. Addition of alcohol gave rise to mobilities between 1.6 and 39 $cm^2V^{-1}s^{-1}$ and electron concentrations between 65.8 and 1.93 $\times$ 10^{20} cm^{-3} for films with thicknesses between 460 and 1220 nm[21]. Variation of methanol content also resulted in high mobilities ($\sim$55 $cm^2V^{-1}s^{-1}$), but very low carrier concentrations ($<4 \times 10^{18}$ cm^3) for films with high thicknesses (>600 nm)[22].

Although great efforts have been made, the mobility improvement is generally accompanied by reduction of carrier density, leading to no net enhancement of conductivity. As a matter of fact, effective methods for improving the optical and electrical properties, specifically, the carrier density and mobility simultaneously are still lacking. In this study, we report a new method for improving mobility and conductivity without sacrificing the carrier density and transparency. Our study is primarily focused on FTO films based on the consideration that FTO is frequently used as an alternative to ITO due to the high cost of the rare element of indium, especially when chemical and electrical stability at elevated temperatures is required for device fabrication or application[23,24]. We particularly investigate the relationship between the electrical property and texture development of FTO thin films at an identical low thickness of 300 nm. The films were deposited from a CVD method by using Dimethyltin Dichloride (DMTDC) and Trifluoroacetic acid (TFAA) as Sn and F precursors, respectively, and the development of different textures was achieved with additions of different additives (water, ethanol, acetylacetone-ACAC, 2,2,6,6-Tetramethylheptane-3,5-dione-TMHD and N,N,N′,N′-tetramethylethylenediamine-TMEDA). It will be shown that texture variation influenced the mobility and thus the conductivity. Specifically, strengthening (200) but weakening (110) preferred orientation enhances carrier mobility with the carrier concentration maintained at a constant high level.

Results

Optical property. All the results are described for the FTO thin films with the same thickness of about 300 nm ($\pm$20 nm). This is to minimize the possible effects of thickness on transmittance, conductivity, grain size and surface roughness. At such a thickness, all the films with or without the additions of the different additives showed a transmittance of 80–85% in the visible light region (Fig. 1). The maximum transmittance of all samples was up to 85% at the wavelength of 550 nm. The transmittance changed little with adding ethanol, and decreased slightly with adding ACAC although it still remained higher than 80% in the visible range. At wavelengths higher than 1200 nm, the transmittance became lower than 80%. All these transmittance values include the absorption and reflectance by the glass substrate as well. If the absorption by the glass substrate was subtracted, the transmittances for the films themselves were higher than 90%. The transmittances of all samples shown in Figure 1 are similar, suggesting that the carrier concentrations in these films could remain at a close level.

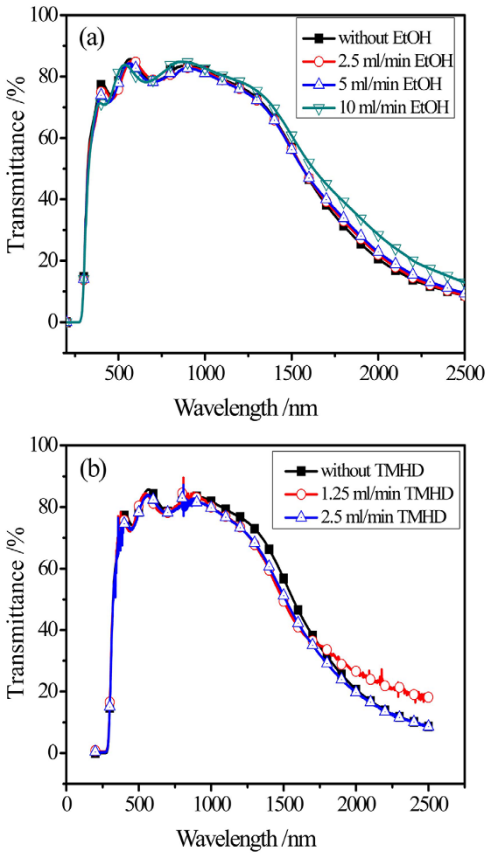

Figure 1 | Typical transmission spectra of FTO thin films deposited with different amounts of ethanol (a) or TMHD (b).

Surface morphology. The surface morphology of the thin film deposited with only water added was relatively uniform and compact, and the grains appeared to be flat. The grain size was generally 100–150 nm (Fig. 2a). The crystal grains changed following the additions of different additives. Pyramidal shapes became prevalent. While the grain size remained unchanged with the addition of ethanol, it notably increased to $\sim$200 nm for all other additives (Fig. 2c–d). Surface morphologies were further revealed by AFM measurements (see Supplementary Fig. S1). All films exhibited surface roughing. The values of surface roughness were approximately 12–14 nm for water and ethanol added films and slightly higher for other additives ($\sim$20 nm). From the baseline condition of only 1.1 mL min^{-1} water added to all other conditions, the growth rate slowed down as revealed by a noticeable increase of deposition time from $\sim$6 to 10–15 sec for achieving films of the same thickness of $\sim$300 nm.

Preferred orientation (PO). The XRD patterns for the cases of water, ethanol and ACAC additions are presented in Figure 3(a, b). It is shown that SnO_2 crystals were polycrystalline and in the tetragonal phase. Peaks for SnO or Sn phases were not observed, indicating that the films were fully oxidized. No appreciable peak shift could be observed, which is reasonable considering that the doping level was relatively small for this system and the anionic radii were rather similar. The major XRD peaks were associated with diffractions of (200), (110), and (211) planes, and their intensities varied for samples deposited with different additives. Without ethanol or ACAC additions, the diffraction of (200) plane was dominant. With ethanol or ACAC additions, the intensity of (110) plane showed apparent increases with increasing the amount of addition, suggesting a possible change in PO of the deposited film.

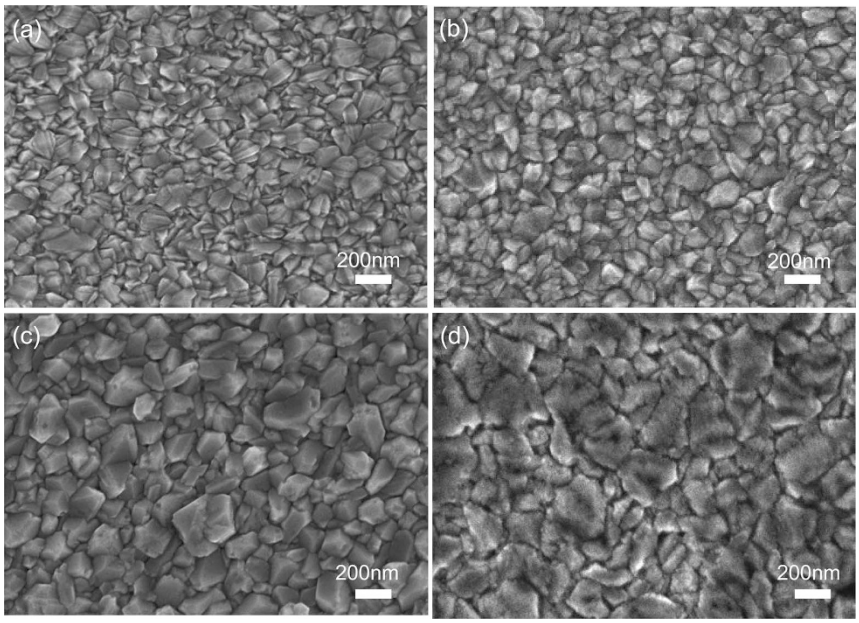

Figure 2 | SEM surface morphologies of FTO thin films with different additives. (a) 1.1 mL min^{-1} H_2O, (b) 5 mL min^{-1} ethanol, (c) 5 mL min^{-1} TMEDA, (d) 5 mL min^{-1} ACAC.

The feature of the PO of a thin film can be quantified by the texture coefficient (TC) which is calculated from the XRD of (hkl) plane as follows[25]:

$$TC_{(hkl)} = \frac{\frac{I_{(hkl)}}{I_{0(hkl)}}}{\frac{1}{n}\sum_{i=1}^{n}\frac{I_{(hkl)}}{I_{0(hkl)}}}, \quad (1)$$

where I is the measured intensity, I_0 the ASTM standard intensity of the SnO_2 power, and n the number of (hkl) diffraction peaks. From the definition, it is obvious that the deviation of TC from unity is indicative of the presence of a PO of the film along the diffraction plane, implying an enhancement in the number of grains along the plane.

The TC values for the three major diffraction planes of (200), (110) and (211) are depicted in Figure 3(c, d) for different additions of ethanol and ACAC. It is clearly shown that the TC for (200) decreased but that for (110) increased with the additions of ethanol or ACAC. Specifically, the TC for (200) decreased from 1.4 to 0.78 and that for (110) increased from 1.0 to 1.7 in the ethanol case. And the TC for (200) decreased from 1.4 to 0.4 and that for (110) increased from 1.0 to 3.2 in the ACAC case. The TC for (211) also decreased with the additions but remained almost constant with

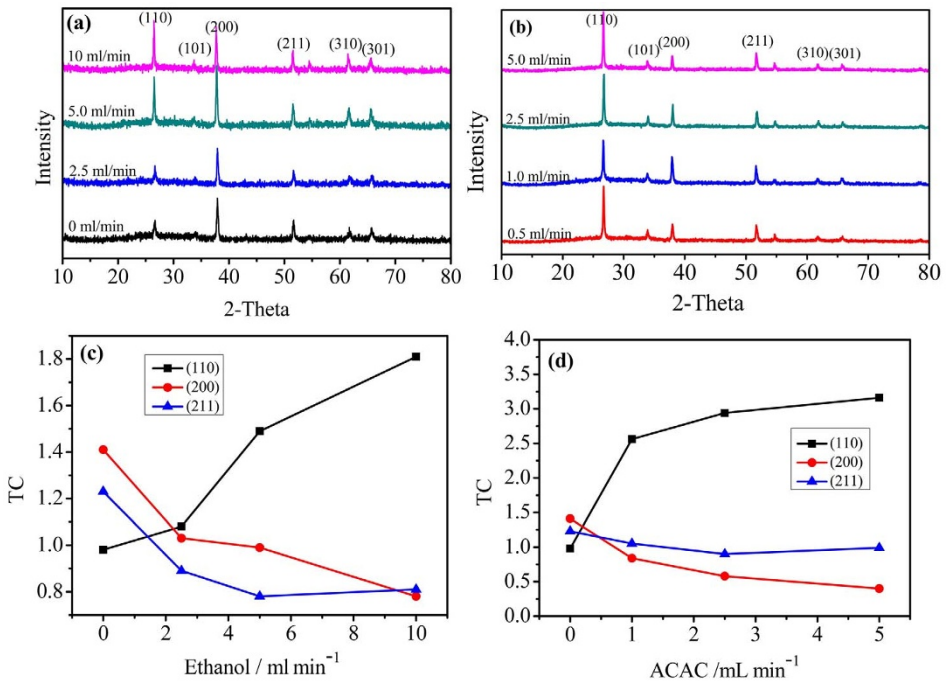

Figure 3 | XRD patterns of FTO thin films with different additions of ethanol (a) and ACAC (b), and influences of additions of ethanol (c) and ACAC (d) on texture coefficient TC.

further additions. These TC results suggest that (200) was substituted by (110) as the PO with the additions of ethanol and ACAC. Such a change was also observed for other additives (see Supplementary Figs. S2–S5).

Electrical property. All the measurements of sheet resistance R_s of the prepared thin films were conducted in the region of the same thickness of ~300 nm. With only water added, R_s was about 14 Ω/□. As ethanol was added in, R_s increased to 20, 25, and 36 Ω/□ for ethanol additions at 2.5, 5 and 10 mL min^{-1}, respectively. When ACAC was added at 0.5 mL min^{-1}, R_s was ~19 Ω/□, being similar to the sample without ACAC addition. However, as the addition increased to 2.5 and 5 mL min^{-1}, R_s increased to as high as 220 and 690 Ω/□, respectively. For TMHD and TMEDA cases, R_s lay between those for ethanol and ACAC cases.

The variations of resistivity (ρ) and conductivity (κ) measured by Hall effect system are shown in Figure 4(a, b) for the cases of water, ethanol and ACAC additions. Generally, ρ increased with the additions of ethanol and ACAC. While for the ethanol case, ρ increased from 5×10^{-4} to 1.4×10^{-3} Ω cm, it went up to 2×10^{-2} Ω cm for the ACAC case. Data for carrier concentration N and mobility μ with different amounts of additions are also available from Hall effect measurements, and they are presented in Figure 4(c, d). As shown, for the case of ethanol addition, N changed only slightly from 4.45 to 3.77×10^{20} cm^{-3}, but μ from 28.5 to 11.3 $cm^2V^{-1}s^{-1}$. For the case of ACAC addition, N again varied little from 4.45 to 4.73×10^{20} cm^{-3}, but μ largely from 28.5 to 0.65 $cm^2V^{-1}s^{-1}$. So μ might be the main factor which affected the resistivity, and the contribution of N might be relatively minor when ethanol or ACAC was added. Nevertheless, for the cases of TMHD and TMEDA cases, both N and μ changed (see Supplementary Fig. S6), and they could affect the resistivity at the same time.

The carrier concentration is affected primarily by fluorine concentration in FTO thin films. This concentration was measured by ToF-SIMS. Figure 5 shows the variations of fluorine concentration with sputter time (that is, the film thickness). Generally, F concentrations show wavy variations with thickness. For the additions of either ethanol or ACAC, the variations are overlapped and do not show a consistent increase or decrease with increasing the addition. Thus, it could be concluded that fluorine concentration remained almost unchanged even though different amounts of ethanol or ACAC were added. This observation is in agreement with the observation that N stayed at the same level for different additions.

Correlation between ρ and TC. Since the electrical conductivity κ (or the reciprocal of resistivity ρ) and texture coefficient TC vary with the amount of addition, the correlation between κ and TC is presented in Figure 6(a, b). All samples are included for which Hall effect and XRD results are available. It is clearly shown that κ decreases with increasing TC(110), but increases with increasing TC(200). Similar correlations can be illustrated between sheet resistance R_s and TC by using all available data (see Supplementary Fig. S7). Data scattering can be narrowed for sheet resistance plotted against the ratio of TC(200)/TC(110), again suggesting the concurrent effects of these POs on electrical property.

Since κ is related with two variables, namely, N and μ, it is necessary to know which variable or whether both variables are dependent upon texture coefficient. As shown in Figure 4(c, d), for ethanol and ACAC additions, N varied within a very narrow range (from 3.77 to 4.73×10^{20} cm^{-3}). Thus, N is almost independent of the additions

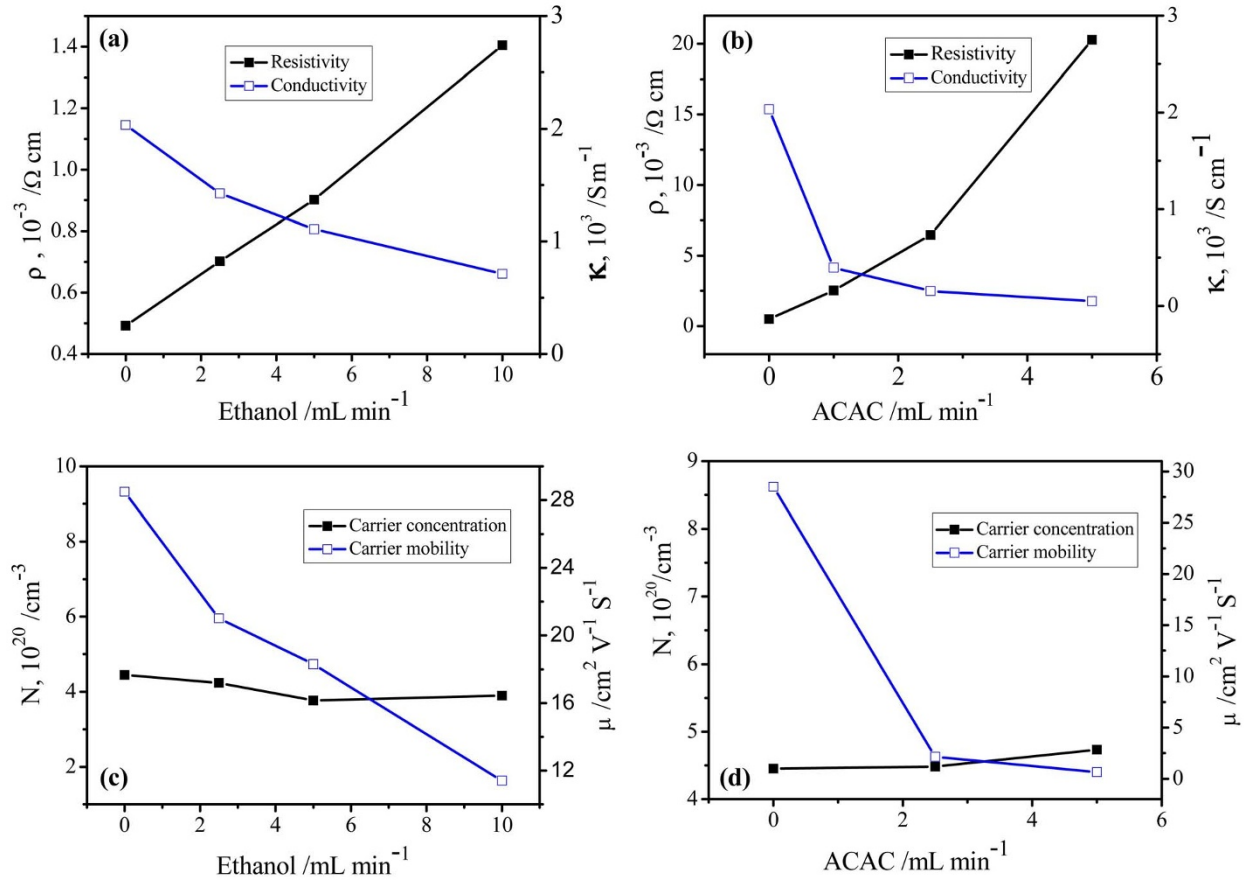

Figure 4 | Variations of resistivity ρ and conductivity κ with additions of ethanol (a) and ACAC (b), and carrier concentration N and mobility μ with additions of ethanol (c) and ACAC (d).

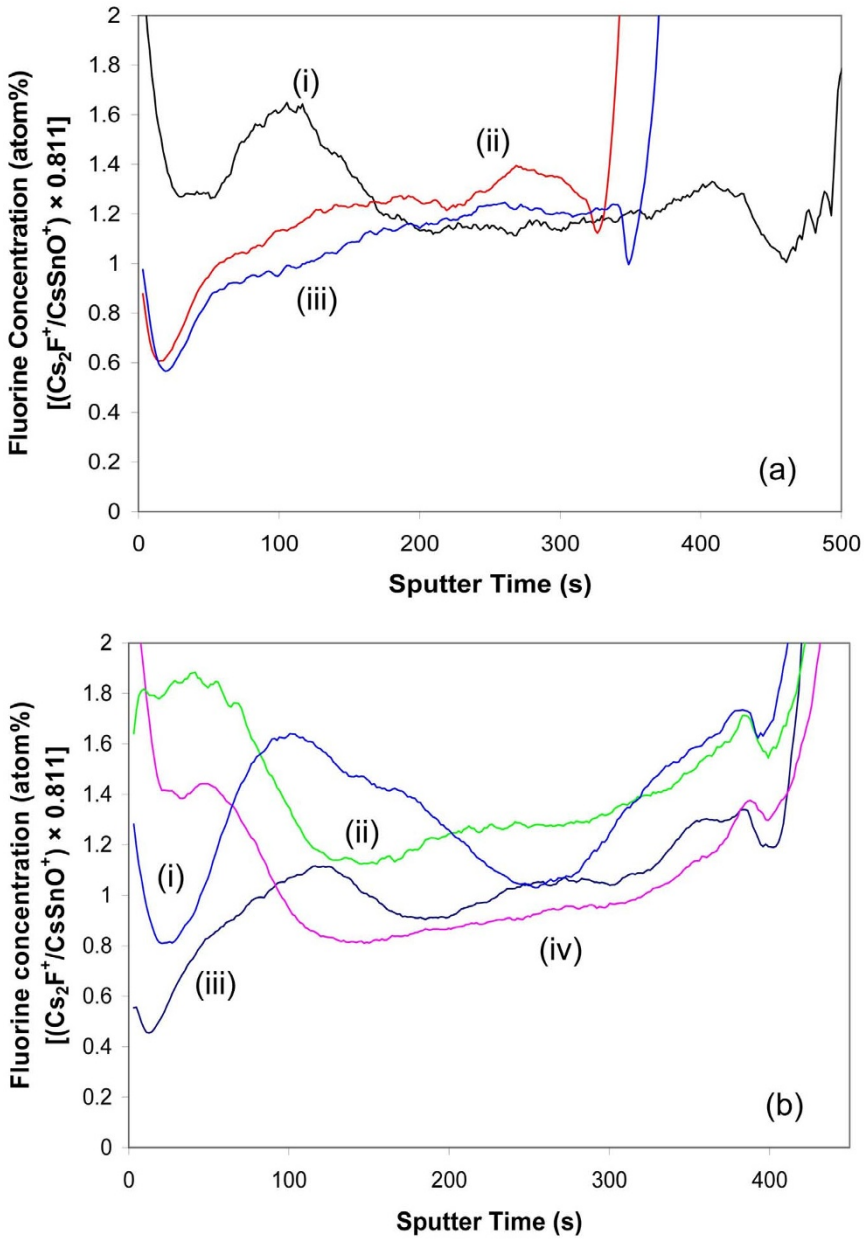

Figure 5 | Variations of fluorine concentration with additions of ethanol (a) [(i): 0, (ii): 2.5, (iii): 10 mL min^{-1}] and ACAC (b) [(i): 5, (ii): 2.5, (iii): 0, (iv): 1 mL min^{-1}].

and thus the texture coefficient. Under this special circumstance, μ is plotted against TC in Figure 6(c, d). A clear negative dependence of μ upon TC(110) and positive dependence upon TC(200) are observed.

Discussion

The prepared films exhibited POs along (200) and (110) planes. Their origins may be considered in terms of periodic band chains (PBC) theory[26]. According to this theory, the external forms of crystals are controlled by PBCs. That is, based on the number of PBCs parallel to the face (hkl), the different faces of SnO_2 can be classified as one of the three faces, flat (F), stepped (S) and kinked (K). F faces are parallel to at least two PBCs, and have surface atoms strongly bound to each other. These faces are little reactive with the arriving atoms. S faces are parallel to only one PBC, and K faces parallel to none. These faces are highly reactive and integrate easily the arriving growth units because they are cut by plenty of unsaturated bonds. For SnO_2, the F and K faces are of great interest, since they are composed of (101) and (111) crystal planes, respectively[27]. F{101} and K{110} faces are polar, which consist of only tin atoms or only oxygen atoms, while F{110} faces are less polar because they are comprised of both tin and oxygen atoms.

The occurrence of a specific growth direction depends upon the precursor materials used for deposition and the thermodynamics of deposition conditions. The prominent (200) growth may be observed for a few reasons. First, (111) K-planes are highly reactive, and can grow at a fast rate as long as sufficient growth atoms are provided. (200) preferred growth was observed to arise from a higher growth rate as a consequence of higher precursor concentration[28,29]. This cannot be changed by even heavy fluorine doping[12]. Second, the orientation with minimum interfacial energy is favored. For tetragonal rutile SnO_2, [200] orientation has a low atomic density and a minimum interfacial energy[30,31]. Hence, the gradual increase of the prominence of [200] is anticipated. Third, the change in preferred orientation from (110) to (200) may be promoted in the presence of halogen-rich gases. As TFAA dissolved in H_2O was introduced for F doping, these polar molecules could adsorb on polar (101) F-planes

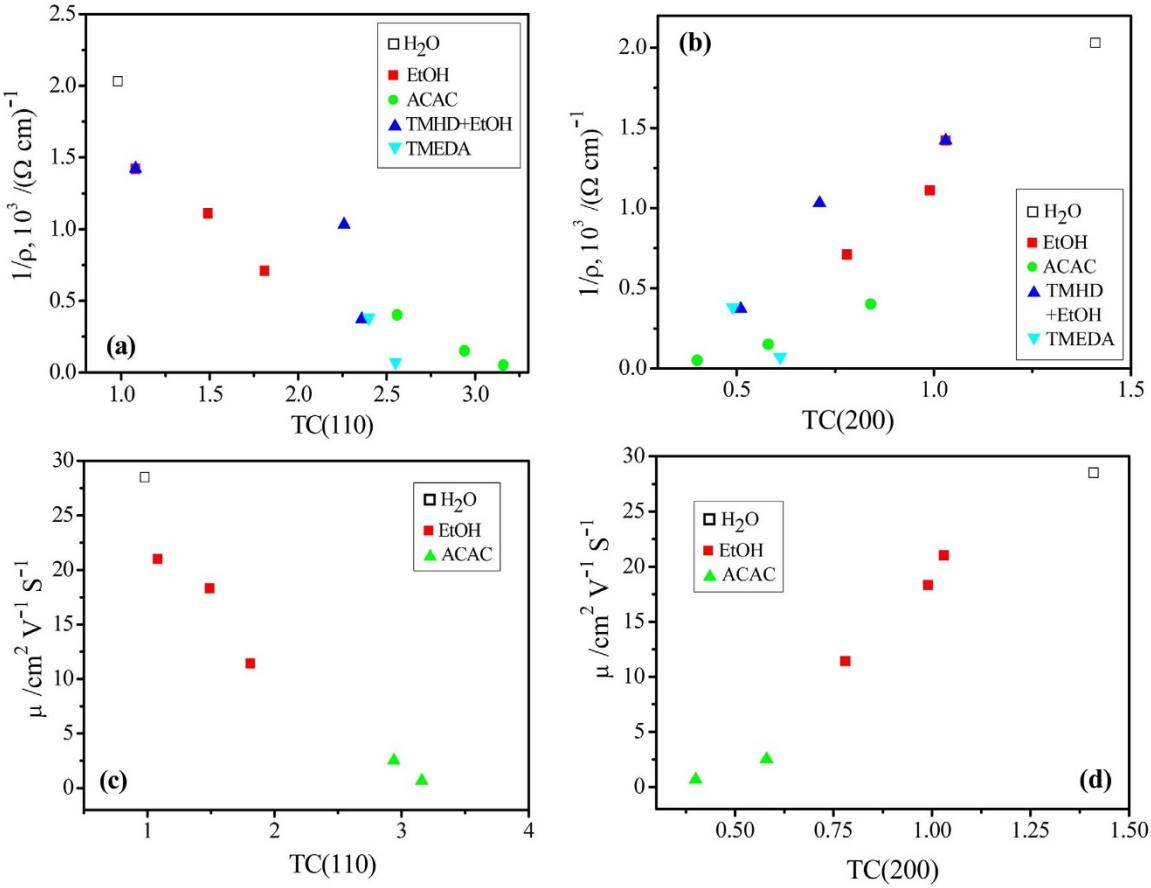

Figure 6 | Variations of resistivity ρ with texture coefficients TC of (110) (a) and (200) planes (b), and carrier mobility μ with texture coefficients TC of (110) (a) and (200) planes (b) at a constant carrier concentration.

and slow down their growth. This might lead to the SnO_2 crystals faceted exclusively by K faces with (200) PO. Favorable effect of the presence of halogen-rich gases on the development of (200) PO has also been reported in the literature[27,32–34]. Addition of HCl or NH_4F maintained the (200) PO in the film, even at the initial stage of deposition[35]. As ethanol or other additives were added without changing other experimental parameters such as Sn and F precursor feeding rates, the actual concentrations of the precursors in the reactants were reduced. The consequences are that less HF molecules adsorbed on polar F-(101) planes, and fewer atoms were supplied to the reactive K-(111) planes within a unit deposition time. All these could have promoted the growth of F-(101) planes and thus (110) PO.

The present FTO films showed evident POs for all additives and the electrical property appeared positively or negatively related to the development of (200) or (110) PO, respectively. A clear variation of conductivity with (200) PO was also observed in some previous studies regardless of the approach used to induce the switch of the PO from (110) to (200)[27,29,32–35]. But the observations were made for films with different thicknesses and different carrier concentrations. It was not possible to correlate the change of PO with the change of conductivity directly. In the present study, however, the films made from inclusions of H_2O, ethanol and ACAC additives had similar carrier concentrations and the same thickness. Thus, it is possible to identify that the change of conductivity is related to the change of carrier mobility and the change of carrier mobility to the change of PO.

The dependence of the carrier mobility upon PO in the form of TC may be related to the carrier scattering mechanism in the present films. It is well known that Hall mobility in doped semiconductors is usually limited by two major scattering mechanisms: grain boundary scattering and ionized impurity scattering[1]. Grain boundaries present a kind of discontinuity in polycrystalline thin films. A space charge region formed around them results in a potential barrier scattering the crossing electrons and thus reducing their mobility. Such scattering can affect the overall TCO mobility only if the grain size is close to the mean free path of the charge carriers.

The mean free path is calculated by the following equation[36]:

$$L = h/(2e)\ (3N/\pi)^{1/3}\mu, \qquad (2)$$

where h is Plank's constant, e is the electron charge (the fundamental charge of an electron is 1.602×10^{-19} C). For the present water, ethanol and ACAC samples with $N = 4–5 \times 10^{20}$ cm^{-3} and $\mu <$ 29 cm^2 V^{-1} s^{-1}, L is < 4 nm. This mean free path is considerably shorter than the grain sizes of the present films (tens to hundreds nanometers). Therefore, Hall mobility is unlikely to be limited by the grain boundary scattering.

The film thickness is an important parameter; many studies show that the electrical and morphological properties of TCO films are highly dependent on the thickness[35,37]. An increase in mobility with thickness can generally be related to an increase in grain size[38] or density[33] because of reduction of the total interfacial grain boundary surface area. As a matter of fact for the present experiments, the grain size for ACAC added films was larger than ethanol and water added ones, but the mobility was much lower.

Long-range electrostatic fields are present around intentional dopants and defects such as interstitials and vacancies. These fields deflect crossing free carriers. Such ionized impurity scattering becomes dominant for electron concentrations above 10^{19} cm^{-3}. Control of Hall mobility by ionized impurity scattering was reported before as evidenced by a mobility enhancement with carrier concentration reduction due to grain size and film thickness increases

achieved by post heat treatment or deposition at high temperature[35]. But, the present measurements were made on films of the same thickness (~300 nm), and showed the same carrier concentration and a smaller mobility for larger-grained ACAC samples than fine-grained ethanol samples.

Furthermore, growth rate effect might come into play for the films with different preferred orientations to change mobility. That is, impurity incorporation may be different for crystals of different orientations growing at different rates. For example, the donor impurity with a low sticking coefficient may evaporate from the surface growing at a slow rate before it gets trapped in the film[39]. The growth of (200) orientation accompanied by large decrease in (110) orientation may result in an increase of the impurity and electron concentration and a decrease of the mobility. But, this is in contrast with the present observations.

Ionized impurity scattering is not responsible for the measured mobility. Other mechanisms must be considered. Lattice scattering is another important source of scattering in typical semiconductor materials. This scattering results from thermal oscillation of atoms and their interference with the moving electrons. It has been theoretically analyzed and experimentally confirmed that in large-grained polycrystalline films, ionized impurity scattering dominated carrier scattering at low temperature but lattice vibration scattering at high temperature (>100 K for ITO and FTO), as long as that a carrier concentration of larger than 5×10^{18} cm^{-3} was maintained[40].

If lattice vibration scattering is predominant, it may vary with crystallographic planes with different atomic densities. It is known that (200) orientation has a low atomic density and (110) orientation has a high atomic density in SnO_2[30,31,33]. Lattice scattering along (200) plane is weaker and thus leads to higher mobility than that along (110) plane. Alternatively, the variation of lattice scattering may result from a change of crystallinity. That is, different growth rates associated with (200) and (110) orientations may lead to different levels of crystallinity. However, the present films showed no indication that the level of crystallinity, appearing in XRD patterns as line broadening, changed with changing preferred orientation.

Although the exact scattering mechanism of the present films needs more investigation, the improvement of Hall mobility with texture development may provide a new direction for future research on FTO and perhaps other TCOs as well. In the present study, experimental parameters were narrowed. Only different additives with various flow rates are supplied into the deposition system. Both TCs for (200) and (110) and resistivity were varied in a much wider range than ever before. A correlation of resistivity with TC was systematically observed. Furthermore, a high level of carrier concentration N was achieved and remained nearly unchanged for the H_2O, ethanol and ACAC cases. As a result, the correlation can be further shown to originate from the dependence of carrier mobility upon TC. The importance of this observation is that the mobility can be increased through controlling (200) PO without sacrificing the carrier concentration and the conductivity. This is significantly different from previous approaches such as post deposition heat treatment and selective doping where high mobility accompanies low carrier concentration and conductivity.

FTO, due to its low cost and chemical and physical stability, has been used to replace ITO. However, the best resistivity for FTO film, $3–4 \times 10^{-4}$ Ω cm, is about a factor of 2–3 higher than that for ITO. The present results suggest that, at high carrier concentration, the resistivity of FTO films may be reduced by increasing Hall mobility through control of (200) PO. Such an approach has the potential to bring the resistivity of FTO films down to the level of ITO.

A few promising methods for control of (200) PO can be proposed, namely, addition of a proper additive, control of doping, control of the chemistry of Sn precursor solution, and use of nucleation layer. The present experimentation revealed that addition of water strengthened (200) PO and reduced the resistivity, but addition of other additives led to suppressive effects. Thus, searching new favorable additives is a straightforward method for promoting (200) PO. Increasing fluorine doping not only enhanced carrier concentration but (200) PO as well[12,41,42]. Antimony doped samples had a higher (200) peak intensity and thus a higher mobility than fluorine doped ones[42]. The use of monobutyltintrichloride (MBTC) or dibutyltin-diacetate (DBTA) as Sn precursor promoted the (200) orientation formed by (111) K-faces when film thickness was increased[33]. FTO films prepared from $SnCl_4$ presented (200) PO, whereas those from $SnCl_2$ showed a disordered PO along (101), (211) and (301) planes[34]. When HCl was added to the $SnCl_2$ precursor solution, the films were highly oriented in (200) direction[42]. The use of a nucleation layer may be one of the most promising ways to control crystallographic orientations of FTO films on heterogeneous substrates. A thin buffer layer of SnO_2 could be deposited prior to the main SnO_2 layer. This buffer layer is such chosen that it serves as both a nucleation layer for determining the predominate orientation of the main layer and a barrier layer to Na-diffusion from the glass. All these approaches should be studied carefully for the purpose of PO control and mobility enhancement. Particular care should be taken in maintaining the carrier density at an acceptable high level.

The texture control may also be used as a general approach for the reduction of the resistivity of current TCO films. Some progress had been made in the reduction in the past two decades. This resulted partially from improvement in deposition technique and better control of the chemistry of the deposition system. However, the resistivity of TCO films appears to have been reduced to a limiting value of $\sim 10^{-4}$ Ω cm. For further reduction to 10^{-5} Ω cm, carrier concentration or mobility or both should be increased. As mentioned above, increasing the carrier concentration to the level of 10×10^{20} cm^{-3} is detrimental to many applications (such as solar cells), because of potential free carrier absorption in the near-infrared range. Therefore, further improvement must necessarily concentrate on approaches to increasing carrier mobility without lowering carrier concentration. For this purpose, texture control, leading to mobility enhancement, may play a unique role, and thus should be explored thoroughly.

In summary, FTO films were prepared with the additions of different additives, including H_2O, ethanol, ACAC, TMHD, and TMEDA. Films with the same thickness were characterized for investigating the effects of these additions on electrical properties. A significant effect of the addition was a substantial variation of film resistivity with PO. Specifically, resistivity increased with strengthening (110) PO and weakening (200) PO. Hall effect measurement further revealed that the observed resistivity increase was due to the decrease of carrier mobility with the development of (110) PO. These results suggest that without destructing high carrier concentration, the electrical conductivity may be improved via carrier mobility by texture control. It is particularly desirable to suppress (110) but promote (200) POs. Such a non-destructive approach is suggested for developing next generation FTO as well as other TCO films with lower than ever resistivity.

Methods

Materials. Ethanol (≥99.7%) was purchased from Sinophram Chemical Reagent Co. DMTDC (>98%), TFAA (99.9%), and other chemicals were purchased from J&K Chemical Ltd, and all water used was deionized by a Millipore system with resistance of 18 MΩ. Soda lime glass was supplied by Nippon Sheet Glass Group. Before it was used as a substrate for FTO films, it was deposited with a layer of SiO_2 of 20 nm thick to impede the migration of alkali metal ions from the glass into the FTO layer.

Synthesis of FTO thin films. FTO thin films were deposited by atmospheric pressure chemical vapor deposition (APCVD). All samples were prepared in a custom built CVD reactor. DMTDC was used as tin precursor. It was vaporized in a bubbler heated at 145°C and carried away by N_2 at a fixed flow rate of 0.98 L min^{-1}. For F doping, TFAA and water were mixed with different volume ratios and injected into a vaporizer heated at 200°C where they were carried away by N_2 at a fixed flow rate of 5 L min^{-1}. For inclusion of additives, they were also fed into this vaporizer. O_2 was

used as oxygen source and supplied at a flow rate of 2.1 L min^{-1} from a separate gas line. All chemicals were mixed in a steel tube and picked up by the main carrier stream of N_2 at a flow rate of 4.5 L min^{-1}. The tube was heated by heater tapes to 200°C to avoid precursor condensation. The mixed gases were delivered to a glass substrate in the reactor in an approximately laminar flow mode. The molar supply rate was calculated from the vapor pressure and flow rate of the nitrogen bubbling gas for each material. When the deposition completed, the mixed gases were directed to an incinerator for decomposition of unused chemicals at 750°C.

In a typical experiment, DMTDC was evaporated in the bubbler at 145°C, and TFAA was dissolved in DI water at a concentration of 30 vol.%. N_2 was used as carrier gas throughout the process. The molar ratio of DMTDC:TFAA:O_2 was fixed at 1 : 10 : 10, then the amount of reagents could be calculated by the vapor pressure, and the flows of N_2 and O_2 were determined. The temperature of the glass substrate was maintained at 600°C. The deposition time was adjusted under the specific reaction conditions to get a target thickness of 300 nm. When the deposition ended, the sample was cooled to <150°C before it was taken out from the reactor.

In order to investigate the effect of preferred orientation on electrical properties, water, ethanol, TMHD, ACAC, and TMEDA were added into the deposition process. The feeding rates of these additives were set at 0, 1.25, 2.5, 5, 10 mL min^{-1}, and the deposition time was adjusted accordingly to make FTO films with the same thickness of ~300 nm. Since water was found to be beneficial to lower resistivity, its flow rate was first optimized to achieve a low resistivity (~1.1 mL min^{-1}). Then, all other additives were supplied at different rates to this water-containing system.

Characterization. Sheet resistance was measured with a SX1944 four-point probe meter with 0.5 mm tip radii and spaced 1 mm apart over a uniform area of coating. The thickness was determined by W-VASE ellipse polarization at the wavelength from 193–1700 nm. The beam diameter was 1 mm. The film thickness was also measured by the method of profilometry. To prepare the needed cross section, 10% HCl and zinc powder were used to mask and etch SnO_2 layers. UV-VIS-NIR spectrophotometer (Varian, Cary 500) was used to investigate the optical properties. Transmission and reflection spectra were measured between 200–2500 nm in 1 nm steps. Transmission was measured with the coated side of the glass against the integrating sphere. The reflection from both sides of the glass was measured. The electrical parameters such as resistivity (ρ), carrier concentration (N) and mobility (μ) at room temperature were measured with Accent HL5500 Hall effect system. An ION-TOF 5 Time of Flight Secondary Ion Mass Spectrometry (ToF-SIMS) instrument was used to obtain a compositional positive ion depth profile for several coatings. The analysis beam was Bi^{3+} and the sputter beam was 1 keV Cs^+ with a beam current of 82+/−2 nA. The sputter beam was rastered over a 200 × 200 micron area, and the bismuth analysis beam was rastered over a 50 × 50 micron area at the centre of the sputtered region.

The surface morphology of FTO films was measured with Hitachi High-Technology S-4800 field emission scanning electron microscope (FE-SEM) at an accelerating voltage of 5 kV. Atomic Force Microscopy (AFM) measurement was performed with Nanoscope IIIa Multimode AFM with the roughness analysis was conducted by the software of Nanoscope 5.30.

The structures of FTO thin films were investigated by X-ray diffraction (XRD) at room temperature with a Rigaku D/max 2550 VB/PC apparatus using Cu Kα radiation (λ = 0.15406 nm) and a graphite monochromator, operated at 40 kV and 100 mA. Diffraction patterns were recorded in the angular range of 10–80° with a step width of 0.02° s^{-1}.

1. Calnan, S. & Tiwari, A. N. High mobility transparent conducting oxide for thin film solar cells. *Thin Solid Films* **518**, 1839–1849 (2010).
2. Porch, A., Morgan, D. V., Perks, R. M., Jones, M. O. & Edwards, P. P. Electromagnetic absorption in transparent conducting films. *J. Appl. Phys.* **95**, 4734–4737 (2004).
3. Porch, A., Morgan, D. V., Perks, R. M., Jones, M. O. & Edwards, P. P. Transparent current spreading layers for optoelectronic devices. *J. Appl. Phys.* **96**, 4211–4218 (2004).
4. Tiwari, A. N. *et al.* CdTe solar cell in a novel configuration. *Prog. Photovolt: Res. Appl.* **12**, 33–38 (2004).
5. Chae, G. S., Soh, H. S., Lee, W. H. & Lee, J. G. Self-passivated copper as a gate electrode in a poly-Si thin film transistor liquid crystal display. *J. Appl. Phys.* **90**, 411–415 (2001).
6. Hamberg, I. & Granqvist, C. G. Evaporated Sn–doped In_2O_3 films: Basic optical properties and applications to energy–efficient windows. *J. Appl. Phys.* **60**, R123–R160 (1986).
7. Granqvist, C. G. & Hultaker, A. Transparent and conducting ITO films: New developments and applications. *Thin Solid Films* **411**, 1–5 (2002).
8. Azens, A. & Granqvist, C. Electrochromic smart windows: energy efficiency and device aspects. *J. Solid State Electrochem.* **7**, 64–68 (2003).
9. King, P. D. C. & Veal, T. D. Conductivity in transparent oxide semiconductors. *J. Phys.: Condens. Matter* **23**, 4214–4230 (2011).
10. Jarzebski, Z. M. & Marton, J. P. Physical properties of SnO_2 materials: I. preparation and defect structure. *J. Electrochem. Soc.* **123**, 199C–205C (1976).
11. Chopra, K. L., Major, S. & Pandya, D. K. Transparent conductors–a status review. *Thin Solid Films* **102**, 1–46 (1983).
12. Agashe, C. & Major, S. S. Effect of heavy doping in SnO_2:F films. *J. Mater. Sci.* **31**, 2965–2969 (1996).
13. Agashe, C. *et al.* Efforts to improve carrier mobility in radio frequency sputtered aluminum doped zinc oxide films. *J. Appl. Phys.* **95**, 1911–1917 (2004).
14. Exarhos, G. J. & Zhou, X. D. Discovery-based design of transparent conducting oxide films. *Thin Solid Films* **515**, 7025–7052 (2007).
15. Shigesato, Y., Takaki, S. & Haranoh, T. Electrical and structural properties of low resistivity tin-doped indium oxide films. *J. Appl. Phys.* **71**, 3356–3364 (1992).
16. Lorenz, M. *et al.* Optical and electrical properties of epitaxial $(Mg, Cd)_xZn_{1-x}O$, ZnO, and ZnO:(Ga, Al) thin films on c-plane sapphire grown by plused laser deposition. *Solid-State Electronics* **47**, 2205–2209 (2003).
17. Ohta, H. *et al.* Highly electrically conductive indium-tin-oxide thin films epitaxially grown on yttria-stabilized zirconia (100) by pulsed-laser deposition. *Appl. Phys. Lett.* **76**, 2740–2742 (2000).
18. Yan, M., Lane, M., Kannewurf, C. R. & Chang, R. P. H. Highly conductive epitaxial CdO thin films prepared by pulsed laser deposition. *Appl. Phys. Lett.* **78**, 2342–2344 (2001).
19. Mizuhashi, M., Gotoh, Y. & Adachi, K. Texture morphology of SnO_2:F films and cell reflectance. *Jpn. J. Appl. Phys.* **27**, 2053–2061 (1988).
20. Isshiki, M. *et al.* Improving mobility of F-doped SnO_2 thin films by introducing temperature gradient during low-pressure chemical vapor deposition. *Jpn. J. Appl. Phys.* **51**, 095801-1–095801-6 (2012).
21. Noor, N. & Parkin, I. P. Enhanced transparent-conducting fluorine-doped tin oxide films formed by aerosol-assisted chemical vapor deposition. *J. Mater. Chem. C* **1**, 984–996 (2013).
22. Deelen, J., van, Volintiru, I., de Graaf, A. & Poodt, P. High mobility tin oxide deposition with methanol addition. In *Photovoltaic Specialists Conference (PVSC), 2011 37th IEEE.* 2826–2828. Seattle, WA. (IEEE, doi: 10.1109/PVSC.2011.6186533).
23. Lee, J. H. & Park, B. O. Transparent conducting ZnO:Al, In and Sn thin films deposited by the sol-gel method. *Thin Solid Films* **426**, 94–99 (2003).
24. Ngamsinlapasathiana, S., Sreethawongb, T., Suzukia, Y. & Yoshikawa, S. Doubled layered ITO/SnO_2 conducting glass for substrate of dye-sensitized solar cells. *Sol. Energy Mater. Sol. Cells* **90**, 2129–2140 (2006).
25. Barret, C. & Massalki, T. B. *Structure of Metals* [204–205] (Pergamon, Oxford, 1980).
26. Hartman, P. *Crystal Growth: an Introduction* [367–402] (North-Holland, Amsterdam, 1973).
27. Smith, A., Laurent, J. M., Smith, D. S., Bonnet, J.-P. & Clemente, R. R. Relation between solution chemistry and morphology of SnO_2-based thin films deposited by a pyrosol process. *Thin Solid Films* **266**, 20–30 (1995).
28. Belanger, D., Dodelet, J. P., Lombos, B. A. & Dickson, J. I. Thickness dependence of transport properties of doped polycrystalline tin oxide films. *J. Electrochem. Soc.: Solid-State Sci. Technol.* **132**, 1398–1405 (1985).
29. Agashe, C., Takwale, M., Bhide, V., Mahamuni, S. & Kulkarni, S. K. Effect of Sn incorporation on the growth mechanism of sprayer SnO_2 films. *J. Appl. Phys.* **70**, 7382–7386 (1991).
30. Fantini, M., Torriani, I. L. & Constantino, C. J. Influence of the substrate on the crystalline properties of sprayed tin dioxide thin films. *J. Cryst. Growth* **74**, 439–442 (1986).
31. Poate, J. M., Tu, K. N. & Mayer, J. W. *Thin Films Inter-diffusion and Reactions* [243–304] (Wiley, New York, 1978).
32. Volintiru, I., Graaf, A. D., Deelen, J. V. & Poodt, P. The influence of methanol addition during the film growth of SnO_2 by atmospheric pressure chemical vapor deposition. *Thin Solid Films* **519**, 6258–6263 (2011).
33. Korotkov, R. Y., Ricou, P. & Farran, A. J. E. Preferred orientations in polycrystalline SnO_2 films grown by atmospheric pressure chemical vapor deposition. *Thin Solid Films* **502**, 79–87 (2006).
34. Gordillo, G., Moreno, L. C., Cruz, W. D. L. & Teheran, P. Preparation and characterization of SnO_2 thin films deposited by spray pyrolysis from $SnCl_2$ and $SnCl_4$ precursors. *Thin Solid Films* **252**, 61–66 (1994).
35. Agashe, C., Hüpkes, J., Schöpe, G. & Berginski, M. Physical properties of highly oriented spray-deposited fluorine-doped tin dioxide films as transparent conductor. *Sol. Energy Mater. Sol. Cells* **93**, 1256–1262 (2009).
36. Yang, J. *et al.* Studies on the structure and electrical properties of F-doped SnO_2 films prepared by APCVD. *Appl. Surf. Sci.* **257**, 10499–10502 (2011).
37. Dong, B. Z., Fang, G. J., Wang, J. F., Guan, W. J. & Zhao, X. Z. Effect of thickness on structure, electrical, and optical properties of ZnO:Al films deposited by pulsed laser deposition. *J. Appl. Phys.* **101**, 033713 (2007).
38. Volintiru, I., Creatore, M., Kniknie, B. J., Spee, C. I. M. A. & Sanden, M. C. M. van de Evolution of the electrical and structure properties during the growth of Al doped ZnO films by remote plasma-enhanced metalorganic chemical vapor deposition. *J. Appl. Phys.* **102**, 043709 (2007).
39. Ohring, M. *Materials Science of Thin Films* [376–385] (Academic Press, New York, 2002).
40. Zhang, D. H. & Ma, H. L. Scattering mechanisms of charge carriers in transparent conducting oxide films. *Appl. Phys. A* **62**, 487–492 (1996).
41. Oshima, M. & Yoshino, K. Electron scattering mechanism of FTO films grown by spray pyrolysis method. *J. Electronic Mater.* **39**, 819–822 (2010).

42. Thangaraju, B. Structural and electrical studies on highly conducting spray deposited fluorine and antimony doped SnO_2 thin films from $SnCl_2$ precursor. *Thin Solid Films* **402**, 71–78 (2002).

Acknowledgments

Financial supports from Pilkington Technology Management Limited, National Natural Science Foundation of China (project #: 51271077 and U1362104) and Shanghai Nanoscience and Nanotechnology Promotion Center (project #: 12 nm 0503300) are greatly acknowledged. Contributions by Drs. T. Manning and Fujisawa Akira during the early stage of this work are greatly thanked.

Author contributions

J.N.W., K.D.S. and P.M.R. designed the research program, J.T.W., X.L.S. and W.W.L. conducted the experimental work, J.N.W. provided the daily supervision, L.P., K.D.S., M.H., K.T. and X.H.Z. joined monthly discussions. J.N.W. and J.T.W. prepared the manuscript, and all authors reviewed it.

Additional information

Supplementary information accompanies this paper at http://www.nature.com/scientificreports

Competing financial interests: The authors declare no competing financial interests.

How to cite this article: Wang, J.T. *et al.* Influence of Preferred Orientation on the Electrical Conductivity of Fluorine-Doped Tin Oxide Films. *Sci. Rep.* **4**, 3679; DOI:10.1038/srep03679 (2014).